Research Article

Arepati Xiakeer, Linxiang Wang*, Munire Maimaiti, Xin Feng, and Mengliang Jiang

Luminescence and temperature-sensing properties of Li⁺, Na⁺, or K⁺, Tm³⁺, and Yb³⁺ co-doped Bi₂WO₆ phosphors

https://doi.org/10.1515/rams-2023-0104 received March 09, 2023; accepted July 17, 2023

Abstract: A series of Li⁺, Na⁺, or K⁺, Tm³⁺, and Yb³⁺ codoped Bi₂WO₆ upconversion phosphors were prepared by a high-temperature solid-phase method at 800°C for 3 h. X-ray diffraction showed that Li⁺, Na⁺, K⁺, Tm³⁺, and Yb³⁺ doping did not affect the orthorhombic structure of the Bi₂WO₆ matrix. Scanning electron microscopy images of the Bi₂WO₆:1% Tm³⁺, 6% Yb³⁺ and 1% Li⁺, 1% Na⁺, or 1% K⁺-doped Bi₂WO₆:1% Tm³⁺, 6% Yb³⁺ samples reveal irregular particles with a 0.5-5 µm particle size range; upon Na⁺ or K⁺ doping, the particle size increases and the particle surface becomes smooth. EDS analysis shows that the above ions are well incorporated into the powder particles. At 298 K, the relative temperature sensitivities are 0.00144, 0.0016, 0.0024, and $0.0018 \,\mathrm{K}^{-1}$ for the 1% Tm^{3+} , 6% Yb^{3+} : $\mathrm{Bi}_2\mathrm{WO}_6$ samples without alkali metal ions and doped with 1% Li⁺, 1% Na⁺, or 1% K⁺ based on the thermally coupled energy level ${}^{3}F_{3}/{}^{3}F_{2}$ characterization temperature. However, under the same conditions, when using the nonthermally coupled level ${}^{3}F_{3}/{}^{1}G_{4}$ characterization temperature, the relative temperature sensitivities of these four samples are 0.0378, 0.0166, 0.046, and 0.0257 K⁻¹, increasing by 26.3, 10.3, 19.1, and 13.9 times, respectively. The relative temperature sensitivities of the 1% Na⁺, 1% Tm³⁺, and 6% Yb³⁺:Bi₂WO₆ samples are the highest at 298 K.

Arepati Xiakeer: College of Physics and Electronic Engineering, Xinjiang Normal University, Urumqi 830054, Xinjiang, China; Xinjiang Key Laboratory of Luminescent Minerals and Optical Functional Materials, Urumqi 830054, Xinjiang, China, e-mail: 1426273440@qq.com Munire Maimaiti, Xin Feng, Mengliang Jiang: College of Physics and Electronic Engineering, Xinjiang Normal University, Urumqi 830054, Xinjiang, China; Xinjiang Key Laboratory of Luminescent Minerals and Optical Functional Materials, Urumqi 830054, Xinjiang, China

Keywords: Tm³⁺, Yb³⁺:Bi₂WO₆ upconversion material, Li⁺, Na⁺, K⁺, doping, thermally coupled energy levels, nonthermally coupled energy levels, relative temperature sensitivity

1 Introduction

Rare earth upconversion luminescent materials have attracted extensive attention from researchers due to their advantages of correspondingly fast, good spatial resolution, and noncontact accurate temperature measurement at the micro/nanoscale, especially near-infrared response upconversion luminescent materials for temperature detection in biological tissues or cells [1,2]. Bi₂WO₆, which has stable physicochemical properties and low phonon energy, can be used as a matrix for upconversion luminescent materials [3]; however, its band gap is 2.7 eV, and therefore, only light below 450 nm is absorbed. The Tm3+ energy levels are abundant, and strong upconversion luminescence can be produced by Yb3+ sensitization, with large absorption in the near-infrared region. Tm³⁺ and Yb³⁺ co-doped luminescent materials and their temperature-sensing properties have attracted much attention from researchers. For example, Thakur et al. [4] prepared Tm3+, Yb3+:YPO4 phosphors by precipitation, and analyzed the luminous intensity ratio of Tm³⁺ for $(^{3}F_{2/3} \rightarrow ^{3}H_{6})/(^{3}H_{4} \rightarrow ^{3}H_{6})$ transitions, and obtained a maximum relative temperature sensitivity of 0.0186 K⁻¹ at 323 K. Yin [5] prepared double lightemitting center Yb3+, Er3+, Tm3+: K3Gd(PO4)2 upconversion luminescent materials by a high-temperature solid-phase method, and the maximum relative temperature measurement sensitivity was 0.0078 K⁻¹ when using the nonthermally coupled energy levels of Er³⁺ (²H_{11/2}, ⁴F_{9/2}). Improving the upconversion luminous efficiency of materials is a way to improve the temperature sensitivity of materials; moreover, suitable metal ion co-doping can effectively improve the luminescence performance and temperature measurement sensitivity of luminescent materials. For example, Zhang et al. [6] used Gd³⁺, Tm³⁺, and Yb³⁺ to co-dope BaWO₄ and found that after Gd³⁺ incorporation, the Tm³⁺

^{*} Corresponding author: Linxiang Wang, College of Physics and Electronic Engineering, Xinjiang Normal University, Urumqi 830054, Xinjiang, China; Xinjiang Key Laboratory of Luminescent Minerals and Optical Functional Materials, Urumqi 830054, Xinjiang, China, e-mail: wanglinxiang23@126.com

2 — Arepati Xiakeer *et al.* DE GRUYTER

blue light (485 nm) was enhanced by 31 times, and the temperature measurement sensitivity reached 0.0119 K⁻¹, which was 8.5 times higher than that without Gd³⁺ doping. Kumar et al. [7] enhanced the luminous efficiency of Tm³⁺, Yb³⁺:YF₃ upconversion luminescent materials by doping with Ca²⁺, and the maximum relative temperature measurement sensitivity of the material at 300 K was 0.00845 K⁻¹. The introduction of Zn²⁺ to Tm³⁺, Yb³⁺: CaGdAl₃O₇ upconversion luminescent materials was found to cause distortion of the local crystal field of Tm³⁺ and enhance the luminescence of Tm³⁺, and the maximum relative temperature sensitivity of the optimized sample reached 0.026 K⁻¹ at 303 K [8]. Meng et al. [9] studied the effect of different Ce³⁺ contents on the luminous intensity of Tm³⁺, Yb³⁺:NaYF₄ and found that Ce³⁺ doping enhanced the blue light of Tm³⁺ at 475 nm, and the absolute sensitivity was as high as 0.035 K⁻¹. Yadav et al. [10] found that when Mg²⁺ was co-doped with a ZnWO₄ phosphor, its luminous intensity increased by two times, and the relative temperature measurement sensitivity was 0.0034 K⁻¹ at 300 K. According to Guan and Li [11], metal ions such as Li⁺, K⁺, and Mg²⁺ can be doped into a phosphor matrix, which plays a sensitizing role by reducing the symmetry of the crystal field around the active ions and effectively improve the dispersion and morphology of the phosphor, thereby improving the luminous efficiency of the luminescent material.

The upconversion luminescence and temperature measurement properties of Tm³+, Yb³+ co-doped in different kinds of matrix materials have been reported, among which the studies on luminescent materials with Bi₂WO6 as the matrix have mainly concentrated on the photocatalytic properties in the visible region. However, the effects of different concentrations of Li⁺, Na⁺, or K⁺ with Tm³+ and Yb³+ co-doping on the upconversion luminescence and temperature measurement properties of synthetic materials under near-infrared excitation have been less reported. Thus, different concentrations of Li⁺, Na⁺, and K⁺ were prepared in Bi₂WO6 phosphors co-doped with Tm³+ and Yb³+ by a high-temperature solid-phase method to study the effects of doped ions on the microstructure, upconversion luminescence, and temperature sensing properties of synthetic materials.

2 Experimental methods

In previous experiments, when the Tm^{3+} and Yb^{3+} doping concentrations were 1 and 6%, respectively, the synthesized Tm^{3+} , Yb^{3+} : Bi_2WO_6 phosphors were found to obtain the strongest upconversion emission, so the Tm^{3+} and Yb^{3+} doping concentrations in this experiment were based on this. xM (x = 1%, 2%, 3%, 4%; $M = Li^+$, Na^+ , K^+) materials were prepared by a high-temperature solid-phase method, in which 1% Tm^{3+} and 6% Yb^{3+} were co-doped with the

Bi₂WO₆ phosphor. All ion doping concentrations in this work are the quantitative concentrations of the substances.

According to the chemical ratio, the raw materials, including $\rm Bi_2O_3$ (99.9%, melting point 825°C), $\rm WO_3$ (99.99%), $\rm Tm_2O_3$ (99.99%), $\rm Yb_2O_3$ (99.99%), $\rm Li_2CO_3$ (99.99%), $\rm Na_2CO_3$ (99.99%) and $\rm K_2CO_3$ (99%), were weighed using an AL104 electronic scale, mixed and ground for 25 min. They were placed in an SX-12-16 muffle furnace at 800°C in air for 3 h, and a series of $\rm Li^+$, $\rm Na^+$, or $\rm K^+$, $\rm Tm^{3+}$, and $\rm Yb^{3+}$ co-doped $\rm Bi_2WO_6$ samples were obtained.

Phase and microstructure analysis was performed using an X-ray diffraction (XRD) diffractometer (Tsushima XRD-6100, Japan). The morphology, size, and dispersion of the synthesized sample were observed using scanning electron microscopy (SEM, JSM-7610FPlus, JEOL), and the surface elements and distribution of the particles were analyzed using mapping. The elemental composition, content, and distribution in the sample were analyzed using energydispersive X-ray spectroscopy (EDS, X-Max50, Oxford, UK). A 980 nm excitation light source was used, and the upconversion emission spectra of samples at different ambient temperatures were measured with a full-featured steady-state/ transient luminescence spectrometer (FLS920, Edinburgh, UK). Sample heating was achieved using a spectrometer (model FLS980) with high temperature fittings. The temperature control range for sample heating was 298-573 K. All instruments were calibrated prior to use, and initial measurements were taken at room temperature.

3 Experimental results and discussion

3.1 XRD characterization

Figure 1 shows the XRD patterns of 1% Tm^{3+} and 6% Yb^{3+} : Bi_2WO_6 and 1% Li^+ , Na^+ , or K^+ co-doped with 1% Tm^{3+} and 6% Yb^{3+} Bi_2WO_6 samples, with 1% Tm^{3+} and 6% Yb^{3+} : Bi_2WO_6 prepared by the high-temperature solid-phase method with calcination at 800°C for 3 h. Figure 1 shows that the diffraction peak positions of the series of powders synthesized by calcination at 800°C for 3 h are consistent with those of the Bi_2WO_6 standard card PDF#39-0256, and no other peaks are found. The doping of Li^+ , Na^+ , K^+ , Tm^{3+} , and Yb^{3+} basically does not change the orthogonal crystal structure of the Bi_2WO_6 matrix, which indicates that the doped ions partially replace Bi^{3+} or are located in the gaps.

Co-doping of Li⁺, Na⁺, or K⁺ with Tm³⁺ and Yb³⁺ shifted the main diffraction peak (131) of the sample $2d\sin\theta = n\lambda$, as

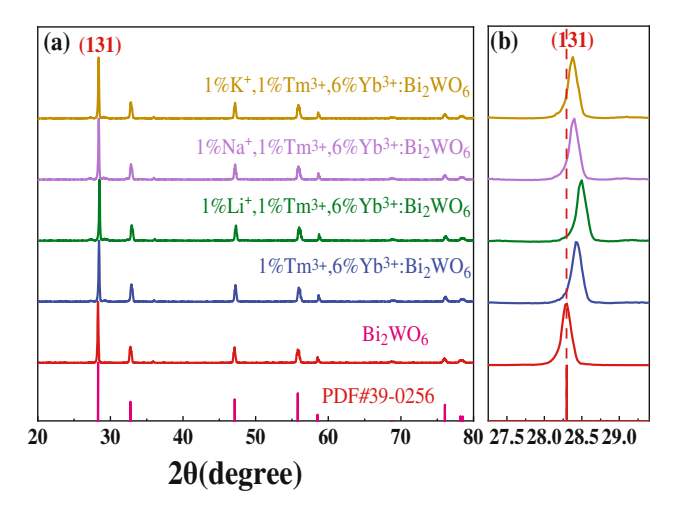


Figure 1: XRD patterns for (a) Li⁺, Na⁺, K⁺, Tm³⁺ and Yb³⁺ co-doped Bi₂WO₆ samples; (b) position comparison of the main diffraction peak (131).

shown in Figure 1(b). With the doping of 1% $\rm Tm^{3+}$ and 6% $\rm Yb^{3+}$, the main (131) diffraction peak of the sample shifted to a larger angle, and after doping with 1% $\rm Li^+$, the diffraction peak shifted more significantly to a larger angle; however, after co-doping with 1% $\rm Na^+$ or $\rm K^+$, the main diffraction peak of the sample shifted to a smaller angle. Due to the same coordination environment, the radius of each metal ion was compared: ($\rm rLi^+$ = 0.076 nm) < ($\rm rYb^{3+}$ = 0.0868 nm) < ($\rm rTm^{3+}$ = 0.088 nm) < ($\rm rNa^+$ = 0.102 nm) < ($\rm rBi^{3+}$ = 0.103 nm) < ($\rm rK^+$ = 0.138 nm). When the small-radius $\rm Tm^{3+}$ and $\rm Yb^{3+}$ dopants replace large-radius $\rm Bi^{3+}$, the unit cell size decreases and

the crystal plane spacing decreases. According to the Bragg equation $(2d\sin\theta = n\lambda, n)$: diffraction order, λ : incident X-ray wavelength, θ : diffraction angle, d: crystal plane spacing), when n and λ are unchanged and the crystal plane spacing decreases, $\sin \theta$ increases; at this time, the diffraction angle θ increases and the diffraction peak shifts to a larger angle. If Li⁺, with the smallest cation radius, replaces Bi³⁺ with a large radius, then the lattice shrinks, the crystal plane spacing decreases, and the diffraction peak shifts to a larger angle. Compared with Na+, the Yb3+ and Tm3+ dopants, Li+ with smaller radii more easily enters the lattice to replace the large-radius Bi³⁺. When Na⁺ enters the lattice, most of the gaps are filled. If a small amount of Na⁺ replaces Bi³⁺, because of the close radii for Na⁺ and Bi³⁺, Na⁺ doping has little effect on the crystal plane spacing, so the diffraction peaks of the two samples before and after 1% Na⁺ doping are basically at the same position. The radius of K⁺ ions is greater than the radius of Bi³⁺, and the K⁺ doping not only occurs in the gaps but also replaces Bi³⁺. If a small amount of K⁺ replaces Bi³⁺, then the lattice expands, the surface spacing d increases, the diffraction angle θ decreases, and the diffraction peak shifts to a smaller angle.

3.2 Surface morphology analysis

Figure 2(a)–(d) shows SEM images of phosphors. The SEM images of the $Bi_2WO_6:1\%$ Tm^{3+} , 6% Yb^{3+} and 1% Li^+ , 1% Na^+ , or 1% K^+ -doped $Bi_2WO_6:1\%$ Tm^{3+} , 6% Yb^{3+} samples are

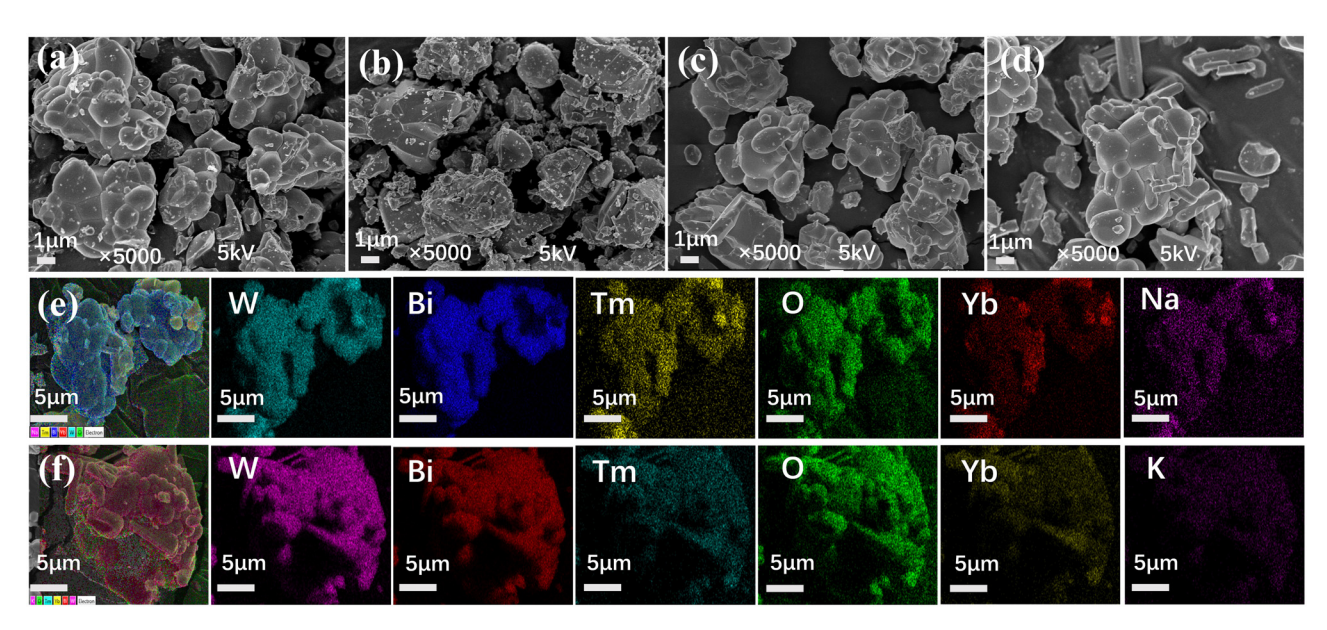


Figure 2: SEM images of Bi_2WO_6 for (a) 1% Tm^{3+} , 6% Yb^{3+} doping; (b) 1% Li^+ , 1% Tm^{3+} , 6% Yb^{3+} doping; (c) 1% Na^+ , 1% Tm^{3+} , 6% Yb^{3+} doping; and (d) 1% K^+ , 1% Tm^{3+} , 6% Yb^{3+} doping; (e) elemental map of 1% Na^+ , 1% Tm^{3+} , 6% Yb^{3+} : Bi_2WO_6 ; and (f) elemental map of the 1% K^+ , 1% Tm^{3+} , 6% Yb^{3+} : Bi_2WO_6 phosphor.

shown in Figure 2(a)–(d). All samples contain irregular particles with a particle size range of $0.5–5\,\mu m$, and all samples exhibit certain aggregation. After doping with Na⁺ or K⁺, the particle size of the sample increases, and the surface of the particles becomes smooth.

By analyzing the surface of 1% Li⁺, 1% Na⁺, or 1% K⁺-doped $\rm Bi_2WO_6$: 1% $\rm Tm^{3+}$, 6% $\rm Yb^{3+}$ samples at 5 μm , the distribution of elements in the surface region of the sample was determined, as shown in Figure 2(e)–(f). The results show that elements such as W, Bi, O, Tm, Yb, Na, and K are evenly distributed on the particle surface (the atomic number of Li is too small to measure). This result indicates that the doped ions Na⁺, K⁺, $\rm Tm^{3+}$, and Yb³⁺ have a good distribution in the matrix material particles.

By analyzing the EDS spectra of the samples, the composition and content of 1% Na $^+$ or 1% K $^+$ -doped Bi $_2$ WO $_6$:1% Tm $^{3+}$, 6% Yb $^{3+}$ samples were determined, as shown in Figure 3(a) and (b). EDS analysis shows that the mass percentage and elemental percentage of various elements in the sample have little deviation from the theoretical values, and the above ions are well incorporated into the powder particles.

3.3 Upconversion emission spectrum

Under near-infrared 980 nm excitation (pump power of 379 mW), the upconversion emission spectra of 1% Tm³⁺ and 6% Yb³⁺:Bi₂WO₆, and the samples with different concentrations of Li⁺, Na⁺, or K⁺ were obtained at room temperature, as shown in Figure 4(a)–(d). Tm³⁺ 478 nm (${}^{1}G_{4} \rightarrow {}^{3}H_{6}$), 650 nm (${}^{1}G_{4} \rightarrow {}^{3}F_{4}$), 685 nm (${}^{3}F_{2} \rightarrow {}^{3}H_{6}$), and 705 nm (${}^{3}F_{3} \rightarrow {}^{3}H_{6}$) emission peaks are exhibited in the 400–745 nm range.

The co-doping of Li^+ , Na^+ , or K^+ ions does not affect the positions of the upconversion emission peaks of Tm^{3+} With increasing Li^+ , Na^+ , or K^+ ion doping, the Tm^{3+} emission intensity in the sample first increases and then decreases. The optimal doping concentrations of Li^+ , Na^+ , and K^+ are 1, 1, and 2%, respectively. When doped with 1% Li^+ , 1% Na^+ , or 2% K^+ , the emission at 685 nm increases by 9.91-, 4.62-, and 1.71-fold, and the emission at 705 nm increases by 9.75-, 5.35-, and 1.76-fold, respectively. The 1% Li^+ -co-doped sample obtains the strongest upconversion luminescence under 980 nm excitation at room temperature.

 ${\rm Li}^+$, ${\rm Na}^+$, or ${\rm K}^+$ co-doping, whether the ions occupy lattice gaps or replace ${\rm Bi}^{3+}$, will cause lattice distortion, and the local crystal field symmetry will be reduced, which is conducive to luminescence enhancement [12]. The melting points of ${\rm Li_2CO_3}$, ${\rm Na_2CO_3}$ and ${\rm K_2CO_3}$ are 723, 851, and 891°C, and the decomposition temperatures are 1,300, 1,744, and 270°C, respectively. When ${\rm K_2CO_3}$ exceeds 270°C, it easily decomposes into ${\rm K_2O}$, and the melting point of ${\rm K_2O}$ is 350°C. In general, the lower the melting point of the flux is, the better the melting effect. Therefore, ${\rm Li_2CO_3}$, ${\rm Na_2CO_3}$, and ${\rm K_2CO_3}$ were used as fluxes, which could reduce the temperature of the reactants. When the melting point of the flux was lower, the powder crystallization performance was better, and the luminescence of the sample was stronger.

An appropriate amount of Li⁺, Na⁺, or K⁺ doping is conducive to promoting luminescence, which is consistent with the results reported by Tuo *et al.* [13]. If Li⁺, Na⁺, or K⁺ enter the lattice, then some of the ions are in the gaps, and some of them substitute Bi³⁺. Based on the ion radius comparison, Li⁺ < Na⁺ < K⁺, smaller-radius Li⁺ more easily replaces Bi³⁺ in the lattice. If a small amount of Li⁺, Na⁺,

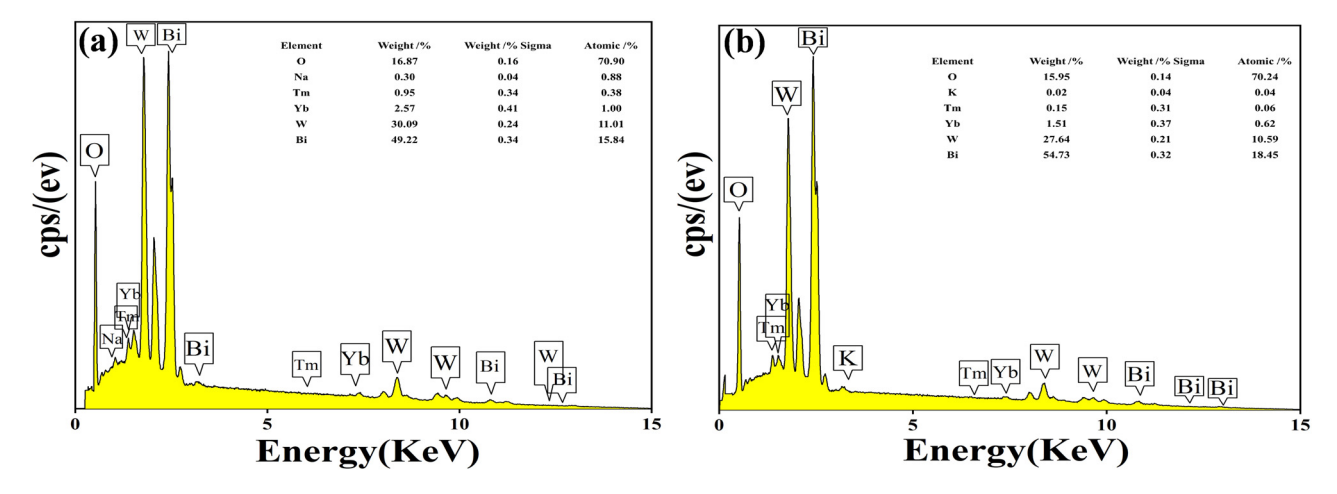


Figure 3: EDS maps for (a) 1% Na⁺, 1% Tm³⁺, 6% Yb³⁺:Bi₂WO₆ and (b) 1% K⁺, 1% Tm³⁺, 6% Yb³⁺:Bi₂WO₆ phosphor.

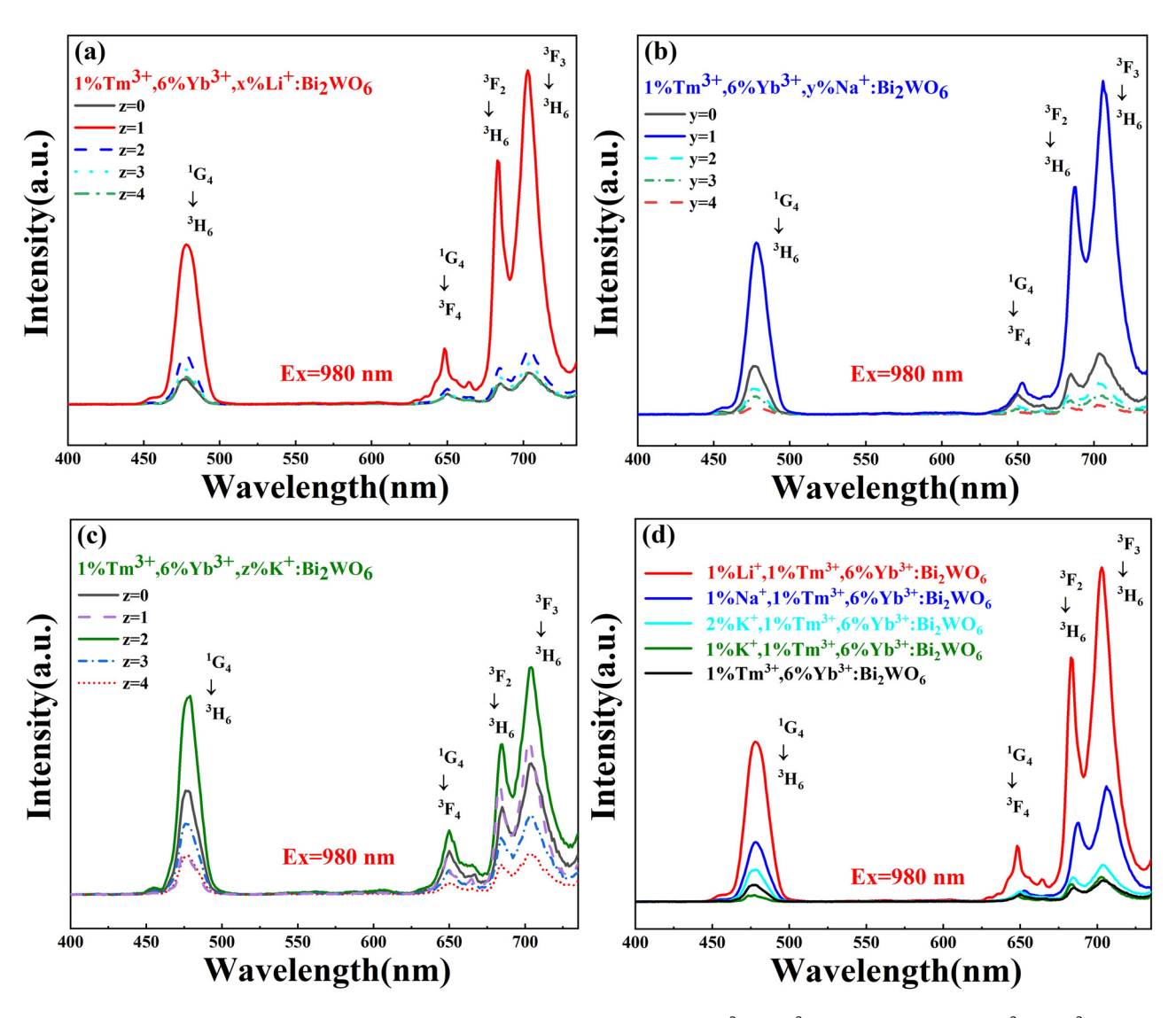


Figure 4: Upconversion emission spectra of samples under 980 nm excitation for (a) 1%Tm³⁺, 6%Yb³⁺, x%Li⁺: Bi₂WO₆; (b) 1%Tm³⁺, 6%Yb³⁺, y%Na⁺: Bi₂WO₆; (c) 1%Tm³⁺, 6%Yb³⁺, z%K⁺: Bi₂WO₆; (d) comparison of luminous intensity on five samples.

or K⁺ replaces Bi³⁺ in the lattice, then according to the conservation of charge, oxygen vacancies will be generated in the grains, and negative electrical defects caused by charge compensation will cause more Tm3+ to enter the lattice, thereby promoting luminescence. When Li⁺, Na⁺, and K⁺ ions are excessively doped, the concentration of nonluminescent centers increases, the probability of crossrelaxation increases, and the probability of nonradiative transition increases, causing luminescence quenching [14].

In this work, the upconversion luminescence intensity order of the samples excited at room temperature under 980 nm (pump power of 379 mW) was as follows: doped 1% Li^+ sample > 1% Na^+ sample > 2% K^+ sample > 1% K^+ sample > undoped alkali metal ion sample.

Figure 5 shows the upconversion emission spectra of 1% Li⁺, Na⁺, or K⁺ co-doped with 1% Tm³⁺ and 6% Yb³⁺ Bi₂WO₆ samples at room temperature under 980 nm excitation (pump power: 100-500 mW). With increasing excitation pump power, the Tm³⁺ emission band intensity in the sample gradually increases.

The double logarithmic light intensity I versus excitation pump power curves are shown in Figure 6, along with the number n of photons absorbed per photon emission process. When the pump power of the excitation light source is less than 199 mW or greater than 400 mW, both the blue and red lights of Tm³⁺ begin to exhibit the phenomenon of the intensity I and excitation power relationship deviating from linearity. Especially when the excitation 6 — Arepati Xiakeer et al. DE GRUYTER

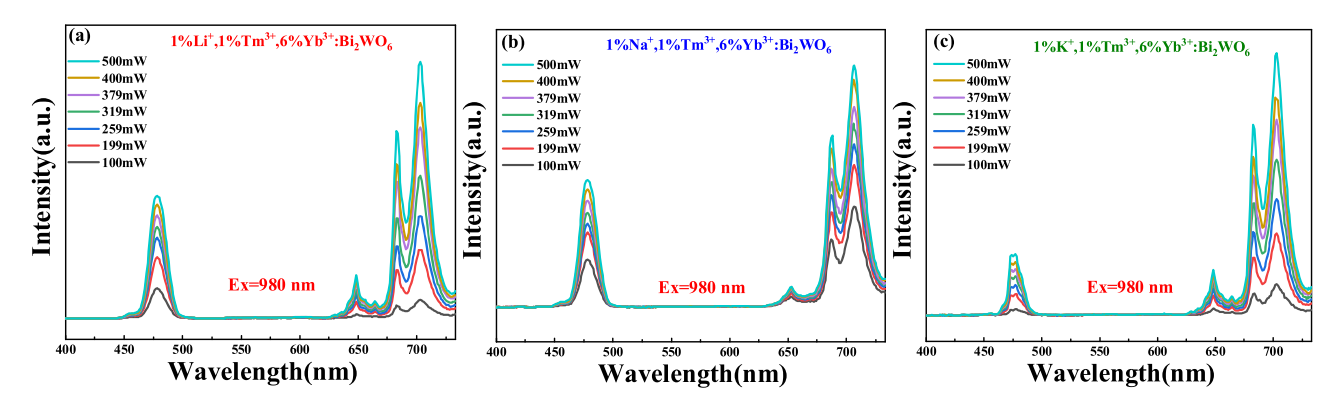


Figure 5: The upconversion luminescence intensity of the sample at the different excitation pump power for (a) $1\%\text{Li}^+$, $1\%\text{Tm}^{3+}$, $6\%\text{Yb}^{3+}$: Bi_2WO_6 ; (b) 1% Na $^+$, $1\%\text{Tm}^{3+}$, $6\%\text{Yb}^{3+}$: Bi_2WO_6 ; (c) $1\%\text{K}^+$, $1\%\text{Tm}^{3+}$, $6\%\text{Yb}^{3+}$: Bi_2WO_6 :

power exceeds 500 mW, the value of n rapidly decreases, seriously deviating from the linear results.

The upconversion of the sample at a certain excitation power was measured, which is proportional to the excitation power P^n based on the luminescence intensity I and the logarithm was taken to analyze the number of absorbed photons. The number of photons n produced by upconversion luminescence after absorption will be affected by the competition between the intermediate ion "upconversion luminescence rate" and "decay rate." Under high-power optical pumping conditions, the value of "n" gradually decreases with increasing power, leading to a "saturation effect." The light intensity I and excitation power P will exhibit a nonlinear relationship, making an accurate determination of the number of absorbed photons required to produce the emission peak difficult. Additionally, under high pump power excitation, the synthesized luminescent material will be affected by the thermal effect caused by the laser, leading to an increase in the probability of nonradiative transitions in the material, resulting in a decrease in the upconversion luminescence and thus affecting the temperature sensitivity of the material. Considering the above factors,

the excitation pump power range selected in this experiment was 199–400 mW.

According to the light intensity I of the four emission bands (478, 650, 685, and 705 nm) and excitation pump power P of the above three samples, the corresponding n values of the four emission peaks of the 1% Li⁺-doped sample were calculated as 1.04, 1.42, 1.69, and 1.65, those of the four emission peaks of the 1% Na⁺-doped sample were 1.13, 1.01, 1.06, and 1.08, and the corresponding n values of the four emission peaks of the 1% K⁺-doped sample were 1.41, 1.18. 1.37, and 1.36. The calculation results show that the four emission peaks of Tm^{3+} in the above three samples are derived from two-photon absorption.

3.4 Temperature-sensing characteristics

Figure 7 shows the upconversion luminescence spectra of $1\% \text{ Li}^+$, Na^+ , or K^+ , $1\% \text{ Tm}^{3+}$, and $6\% \text{ Yb}^{3+}$ co-doped Bi_2WO_6 samples and $1\% \text{ Tm}^{3+}$ and $6\% \text{ Yb}^{3+}$ co-doped Bi_2WO_6 samples under 980 nm excitation (pump power of 379, 400, or 500 mW). The positions of the emission peaks of all the

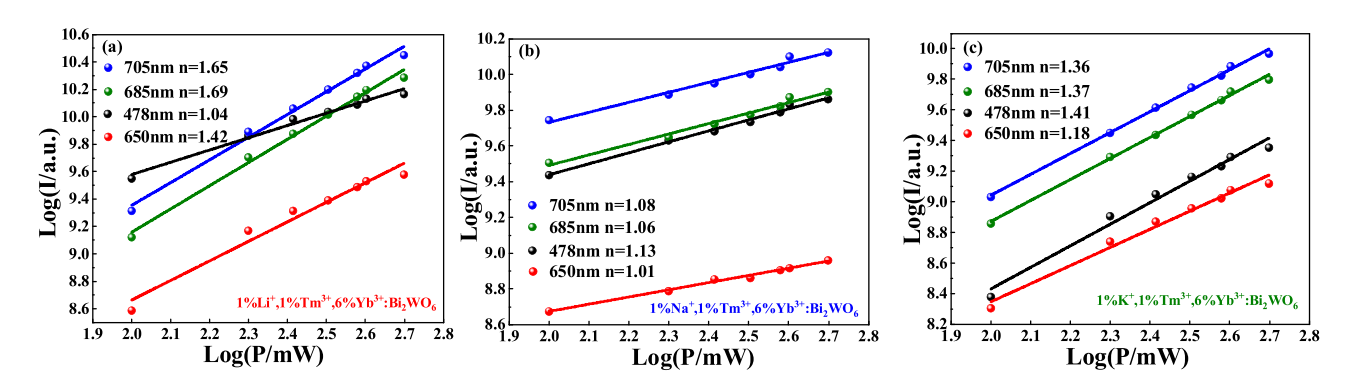


Figure 6: Relationship between the upconversion emission intensity and pump power of samples at room temperature for (a) 1%Li⁺, 1%Tm³⁺, 6%Yb³⁺: Bi₂WO₆; (b) 1%Na⁺, 1%Tm³⁺, 6%Yb³⁺: Bi₂WO₆; (c) 1%K⁺, 1%Tm³⁺, 6%Yb³⁺: Bi₂WO₆.

samples do not change at different temperatures, but the red emission of Tm³⁺ at 650, 685, and 705 nm gradually increases with increasing ambient temperature.

The material will be affected by the thermal effect caused by the high-power laser, resulting in an increase in the probability of nonradiative transitions, and the optical temperature sensitivity of the material is bound to be affected. By comparison, the variable temperature upconversion red light emission intensity of the sample obtained under 379 mW excitation varies more significantly with temperature. Therefore, 908 nm excitation with a pump power of 379 mW was selected for the subsequent studies.

When the pump power is 379 mW, the red luminescence intensity of the samples doped with 1% Li⁺, Na⁺, or K⁺ reaches the maximum value in this temperature range at 573 K, and the green light of the K⁺-doped samples at 478 nm gradually increases with increasing temperature. When the pump power is 400 mW, with increasing temperature, the green light emission of the samples doped with 1% Li⁺ or Na⁺ first increases and then decreases, whereas the green emission of the samples doped with

1% K⁺ increases. When the pump power is 500 mW, with increasing temperature, the green light emission of the samples doped with 1% Li⁺ or K⁺ is basically unchanged, whereas the green emission of the samples doped with 1% Na⁺ is enhanced. For the samples doped with 1% Li⁺, at 573 K, their Tm³⁺ thermally coupled energy levels $^3F_2/^3F_3$ transition to 3H_6 to produce red light emission at 685 and 705 nm that is 86.4 and 75.6 times higher than that of the samples not doped with Li⁺ at 298 K.

In general, the coupling of trivalent rare earth ions and lattice vibration is weak, and the quenching temperature of synthetic materials is higher. When the ambient temperature rises, the lattice vibration intensifies, and the phonon number increases; the more energy the electrons obtain from the lattice vibration, the greater the chance that the energy absorbed by Tm³⁺ will excite the electrons to a high energy level. However, during the heating process, thermal excitation and thermal quenching in the material will compete, but if the quenching temperature of the material is not reached, then the probability of thermal excitation occurring is higher. The experimental results of Figure 7 show that under 980 nm excitation, from

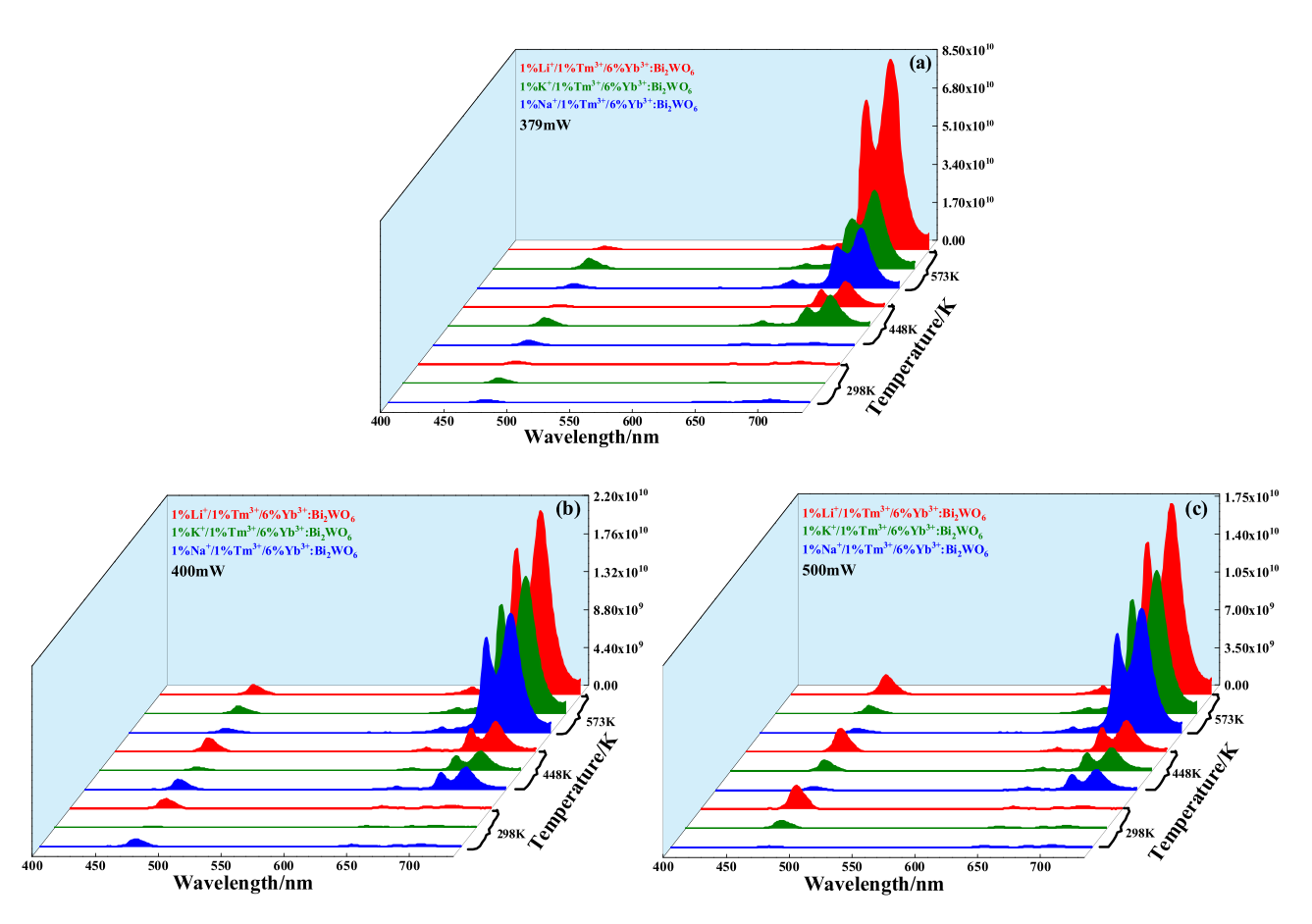


Figure 7: Temperature-dependent upconversion luminescence spectra of Li⁺-, Na⁺-, or K⁺-doped Tm³⁺, Yb³⁺:Bi₂WO₆ samples at (a) 379 mW; (b) 400 mW; (c) 500 mW.

298 to $573\,\mathrm{K}$, the red light emission of all the samples is enhanced, and no luminescence thermal quenching occurs, indicating that the thermal quenching temperature of the material has not been reached at $573\,\mathrm{K}$.

According to the results of Figure 4, at room temperature (980 nm excitation, 379 mW pump power), compared with Na⁺ or K⁺ doping, the 1% Li⁺ doping effect in promoting Tm³⁺ luminescence is more pronounced. As shown in Figure 7, from 298 to 573 K, the luminescence of Li⁺doped synthetic materials is stronger at the same excitation power. Since the thermally coupled levels ${}^{3}F_{3}/{}^{3}F_{2}$ of Tm³⁺ are more sensitive to temperature, for the same increase in temperature, with phonon assistance, the number of particles at the lower energy levels ${}^{3}F_{3}/{}^{3}F_{2}$ will be much higher than the number of particles at the higher energy level ¹G₄. Thus, the probability of ${}^{3}F_{3}/{}^{3}F_{2}$ radiation transition at high temperatures is greater than the probability of ¹G₄ emission, showing 685 and 705 nm emission intensities greater than the 650 nm emission intensity [15]. The position of the ³F₃ energy level is lower than that of ³F₂. Thus, for the same increase in temperature, the number of particles at ${}^{3}F_{3}$ is more than that at ³F₂, and the probability of ³F₃ radiation is greater than the probability of ³F₂ emission; that is, the luminescence at 705 nm is stronger than the luminescence at 685 nm.

The above analysis shows that the melting point and properties of the flux, type, and valence state of doped ions, ion radius, ion concentration, crystal field symmetry, charge compensation, oxygen vacancy formation, ambient temperature, excitation pump power, and other factors will affect the luminescence of the material doped with different metal ions. The main factors affecting them are different, and the luminescence effect of the material differs.

According to Boltzmann distribution theory, under thermal equilibrium conditions, the luminous intensity ratio of two energy levels L_2 (upper energy level, particle number N_2) and L_1 (lower energy level, particle number N_1) can be obtained as a function of the *FIR* and absolute temperature T [16]:

$$FIR = \frac{I_{2j}}{I_{1j}} = \frac{N_2 A_{2j} \omega_{2j}}{N_1 A_{1j} \omega_{1j}} = B \cdot \exp\left(-\frac{\Delta E_{21}}{k_B T}\right)$$
(1)

Here, FIR is the luminous intensity ratio, I_{2j} , I_{1j} , and ΔE_{21} represent the luminous intensities of the upper and lower energy levels, and the difference between the two energy levels, $B = \frac{A_{2j}\omega_{2j}g_2}{A_{1j}\omega_{1j}g_1}$, k_B is the Boltzmann constant, A_{ij} and ω_{ij} are the corresponding spontaneous radiation transition probability and photon angle frequency, and g_2 and g_1 are the degeneracy of energy levels L_2 and L_1 , respectively.

Under 980 nm excitation with 379, 400, and 500 mW excitation pump powers, the ${\rm Tm}^{3+}$ thermally coupled levels ${}^3{\rm F}_3/{}^3{\rm F}_2$ were used to calculate the relative temperature sensitivity $S_{\rm r}$ of the four samples. $S_{\rm r}$ is larger under a 379 mW excitation pump power, so the fitting calculation uses the data measured at a 379 mW pump power.

Figure 8(a)–(d) shows the temperature dependence of fluorescence intensity ratio between 705 and 685 nm in the four samples of $\rm Tm^{3+}$ and $\rm Yb^{3+}$ co-doped $\rm Bi_2WO_6$ and 1% $\rm Li^+$, 1% $\rm Na^+$ or 1% $\rm K^+$ co-doped with $\rm Tm^{3+}$ and $\rm Yb^{3+}$ $\rm Bi_2WO_6$ (980 nm excitation, 379 mW pump power). The relationship of the $\it FIR$ of the $\rm Tm^{3+}$ thermally coupled energy levels ${}^3\rm F_3/^3\rm F_2$ and absolute temperature $\it T$ was fitted. The functional relationship after fitting is as follows:

$$FIR = 1.75 \exp(-123.24/T),$$
 (2)

$$FIR = 0.974 \exp(-144.8/T),$$
 (3)

$$FIR = 5.36 \exp(-162.42/T),$$
 (4)

$$FIR = 4.75 \exp(-217.24/T).$$
 (5)

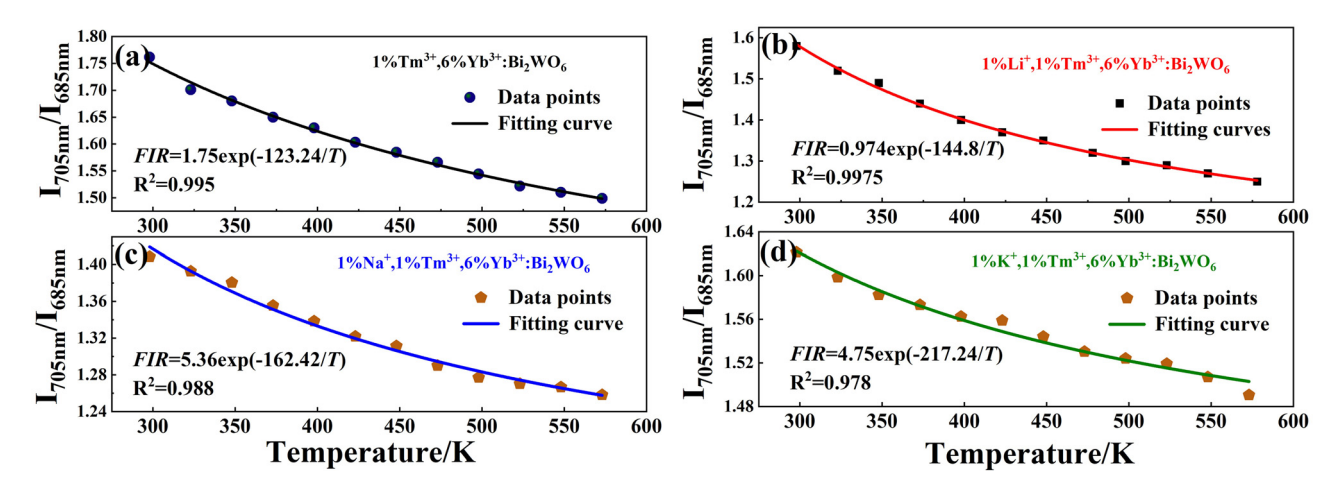


Figure 8: Temperature dependence of fluorescence intensity ratio between 705 and 685 nm *FIR* and the absolute temperature (980 nm excitation, 379 mW pump power). (a) 1%Tm³⁺, 6%Yb³⁺: Bi₂WO₆; (b) 1%Li⁺, 1%Tm³⁺, 6%Yb³⁺: Bi₂WO₆; (c) 1%Na⁺, 1%Tm³⁺, 6%Yb³⁺: Bi₂WO₆; (d) 1%K⁺, 1%Tm³⁺, 6%Yb³⁺: Bi₂WO₆;

According to Zhou *et al.* [17], the absolute temperature measurement sensitivity S_a and the relative temperature measurement sensitivity S_r of a material can be expressed as

$$S_{\rm a} = \left| \frac{{\rm d}FIR}{{\rm d}T} \right|,\tag{6}$$

$$S_{\rm r} = \left| \frac{1}{FIR} \frac{\mathrm{d}FIR}{\mathrm{d}T} \right|,\tag{7}$$

where FIR is the luminous intensity ratio and T is the absolute temperature.

The absolute temperature sensitivity S_a and relative temperature sensitivity S_r of Tm³⁺ and Yb³⁺ co-doped Bi₂WO₆ and 1% Li⁺, Na⁺, or K⁺, Tm³⁺, and Yb³⁺ co-doped Bi_2WO_6 (using the thermally coupled energy level ${}^3F_3/{}^3F_2$ characterization temperature) are shown in Figure 9. The results show that both S_a and S_r decrease with increasing temperature, and, at 298 K, both the S_a and S_r of the four samples show the maximum values. The samples not doped with Li⁺, Na⁺, or K⁺ have maximum S_a and S_r values of 0.00254 and 0.00144 K^{-1} . The maximum S_a and S_r values of the 1% Li⁺-doped samples are 0.0026 and 0.0016 K⁻¹; those for the 1% Na⁺-doped samples are 0.003 and 0.0018 K⁻¹; and those of the 1% K^+ -doped samples are 0.0034 and 0.0024 K^{-1} . Using the thermally coupled energy levels ${}^{3}F_{3}/{}^{3}F_{2}$ to characterize the temperature, the maximum values of S_a and S_r are increased in samples doped with Li⁺, Na⁺, or K⁺ compared with samples not doped with alkali metal ions.

Under the same measurement conditions, the 705 and 650 nm FIR corresponding to the Tm^{3+} nonthermally coupled energy level $^3F_3 \rightarrow ^3H_6$ and $^1G_4 \rightarrow ^3F_4$ transitions in the above four samples was used to characterize the temperature, and the relationship between the nonthermally coupled energy level $^3F_3/^1G_4$ FIR and the absolute

temperature *T* is shown in Figure 10 (980 nm excitation, 379 mW pump power). The functional relationship after fitting is as follows:

$$FIR = 3.14 \exp(-3361.5/T),$$
 (8)

$$FIR = 3.04 \exp(-1482.2/T),$$
 (9)

$$FIR = 3.87 \exp(-4082.1/T),$$
 (10)

$$FIR = 3.77 \exp(-2290.4/T).$$
 (11)

The temperature was characterized by the nonthermally coupled energy levels ${}^3F_3/{}^1G_4$, and the corresponding change laws of S_a and S_r with temperature are shown in Figure 11. By calculating the S_a and S_r of the materials, the results show that the S_a of the samples not doped with Li^+ , Na^+ , or K^+ gradually increases with increasing temperature, and the maximum value of S_a at 573 K is 0.167 K⁻¹. The S_a of the samples doped with 1% Li^+ , Na^+ , or K^+ first increases and then decreases with increasing temperature, and the maximum S_a values are obtained at 548 K, which are 0.196, 0.0977, and 0.476 K⁻¹, respectively. The maximum S_r values of the four samples doped with 1% Li^+ , Na^+ , or K^+ or not doped are obtained at 298 K, which are 0.0378, 0.0166, 0.046, and 0.0257 K⁻¹.

The temperature measurement properties of Tm³⁺ and Yb³⁺ co-doped Bi₂WO₆ with 1% Li⁺, 1% Na⁺ or 1% K⁺ were compared with those of Tm³⁺ and Yb³⁺ co-doped Bi₂WO₆: the experimental results show that the doping of the alkali metal not only improves the upconversion luminescence of Tm³⁺ and Yb³⁺ co-doped Bi₂WO₆ but also improves the temperature measurement sensitivity, especially the sensitivity corresponding to the nonthermally coupled energy levels. For the same sample, under 980 nm excitation with 379 mW pump power, in the 298–573 K temperature range,

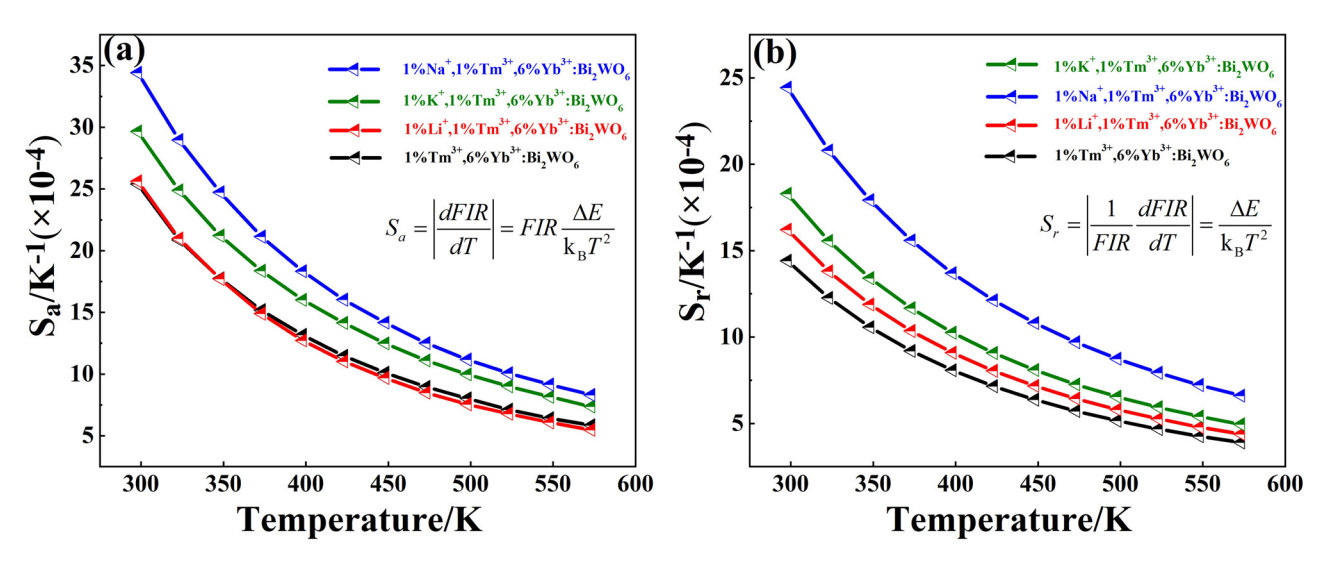


Figure 9: (a) The absolute temperature sensitivity of the sample and (b) the relative temperature sensitivity.

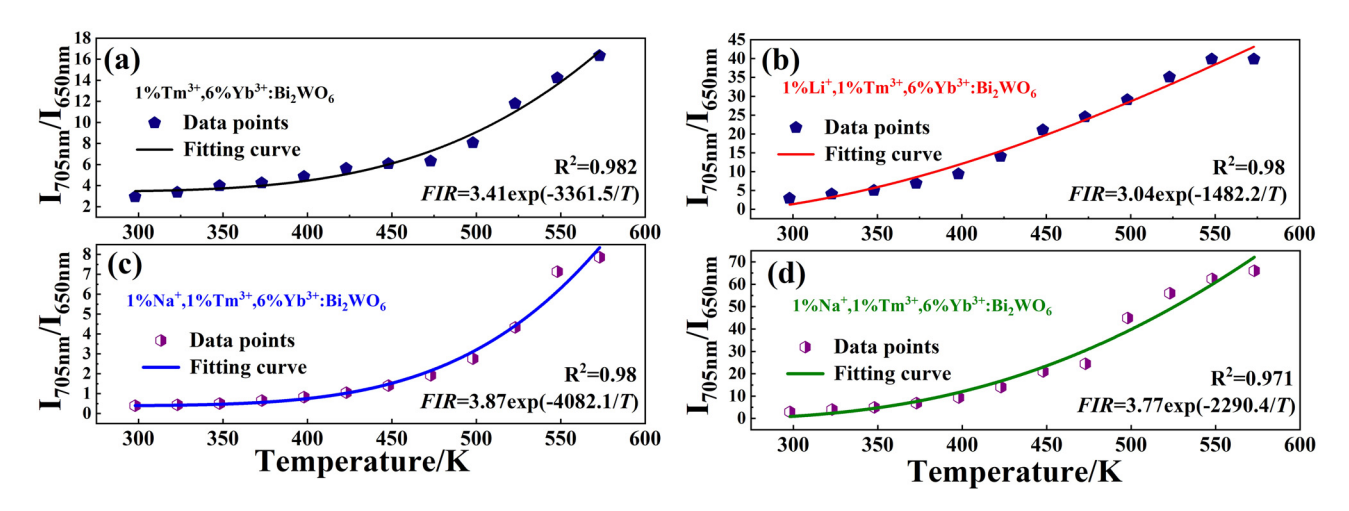


Figure 10: Temperature dependence of the *FIR* of the peaks at 705 and 650 nm generated by a nonthermally coupled energy level pair (980 nm excitation, 379 mW pump power). (a) $1\%\text{Tm}^{3+}$, $6\%\text{Yb}^{3+}$: Bi_2WO_6 ; (b) $1\%\text{Li}^+$, $1\%\text{Tm}^{3+}$, $6\%\text{Yb}^{3+}$: Bi_2WO_6 ; (c) $1\%\text{Na}^+$, $1\%\text{Tm}^{3+}$, $6\%\text{Yb}^{3+}$: Bi_2WO_6 .

compared with the thermally coupled energy level ${}^3F_3/{}^3F_2$ characterization temperature, the maximum relative temperature measurement sensitivity of the material is larger with the nonthermally coupled energy level ${}^3F_3/{}^1G_4$ characterization temperature at 298 K, and the temperature measurement is more accurate.

Table 1 shows the temperature measurement properties of $\rm Tm^{3+}$ and $\rm Yb^{3+}$ doped in different matrix materials and the phosphors synthesized in this work [6,18–23]. Compared with the temperature measurement sensitivity of different matrix materials in the table, the 1% $\rm Na^+$, 1% $\rm Tm^{3+}$, and 6% $\rm Yb^{3+}:Bi_2WO_6$ materials synthesized in this work have a higher maximum relative temperature measurement sensitivity, obtained by using the nonthermally coupled energy level $\rm ^3F_3/^1G_4$ *FIR* in the range of 298–573 K.

4 Conclusion

The $\rm Bi_2WO_6$ series upconversion phosphors with different concentrations of $\rm Li^+$, $\rm Na^+$, $\rm K^+$, $\rm Tm^{3+}$, and $\rm Yb^{3+}$ were prepared by calcination at 800°C for 3 h by a high-temperature solid-phase method. The XRD results showed that the doping of $\rm Li^+$, $\rm Na^+$, $\rm K^+$, $\rm Tm^{3+}$, and $\rm Yb^{3+}$ basically did not change the orthogonal crystal structure of the $\rm Bi_2WO_6$ matrix; after co-doping with 1% $\rm Li^+$, the main (131) diffraction peak shifted to a larger angle, whereas after doping with 1% $\rm Na^+$ or $\rm K^+$, the main diffraction peak of the sample began to shift to a smaller angle. At room temperature, samples doped with 1% $\rm Li^+$, $\rm Na^+$, or 2% $\rm K^+$ emitted 9.91-, 4.62-, and 1.71-fold higher emissions at 685 nm and 9.75-, 5.35-, and 1.76-fold higher emission at 705 than undoped

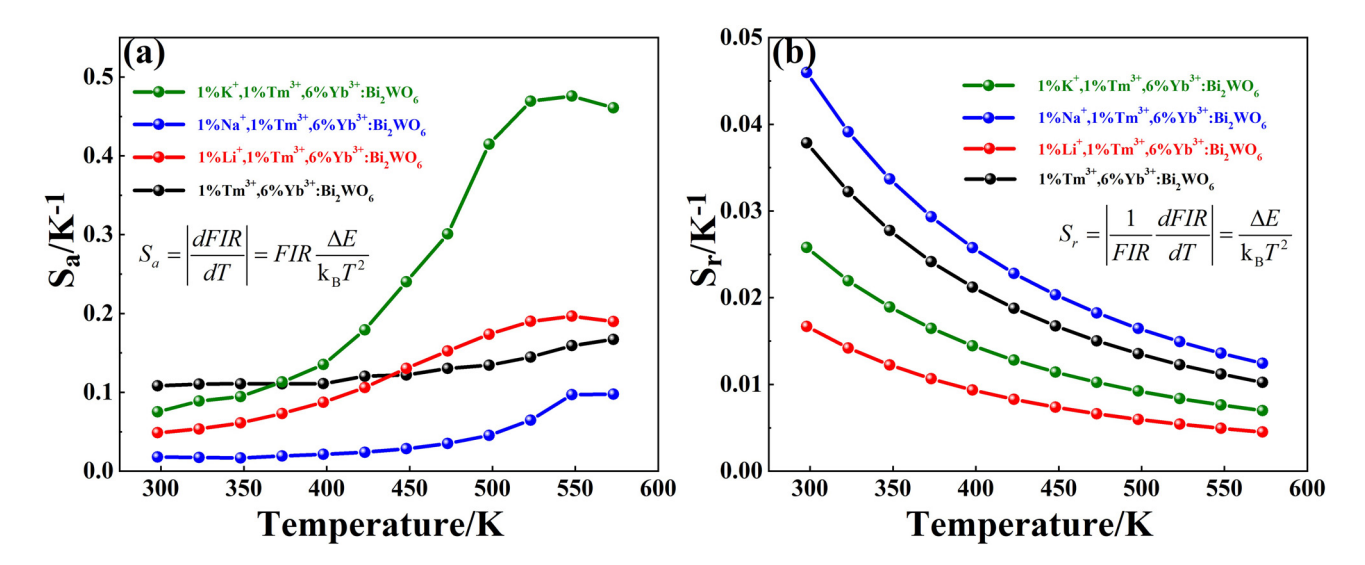


Figure 11: (a) The absolute temperature sensitivity and (b) the relative temperature sensitivity of the nonthermally coupled energy level ${}^{3}F_{3}/{}^{1}G_{4}$ characterization temperature.

Table 1: Comparison of several phosphors for temperature sensors

Host material	Energy level	Temperature range (K)	Temperature range (K) Maximum absolute temperature measurement sensitivity (K ⁻¹)	Maximum relative temperature measurement sensitivity (K^{-1})	Ref.
Tm ³⁺ , Yb ³⁺ -doped borophosphate	${}^{3}F_{2,3}$, ${}^{1}G_{4} \rightarrow {}^{3}H_{6}$ 298–573	298–573	0.1064@573 K	0.0414@298 K	[9]
gid.55 Tm³+, Yb³+:Lu ₂ O ₃	${}^{3}F_{2}, {}^{3}F_{3} \rightarrow {}^{3}H_{6}$	373–973	1	0.0056@535 K	[18]
Tm^{3+} , yb^{3+} :Lu yO_3	${}^{3}F_{2}, {}^{3}F_{3} \rightarrow {}^{3}H_{6}$	223–723	0.00144@723 K	0.00461@516.3 K	[19]
Tm³+, Yb³+:LiNbO₃	$^{3}\text{H}_{4} \rightarrow ^{3}\text{H}_{6}$	80–260	0.037@80 K	0.0125@80 K	[20]
Tm³+, Yb³+:Bi,Ti,O,	$^{3}F_{3}, ^{3}H_{4} \rightarrow ^{3}H_{6}$	300–505	ı	0.024@300 K	[21]
Tm^{3+} , Yb^{3+} :CaWO ₄	${}^{3}F_{2}, {}^{3}F_{3} \rightarrow {}^{3}H_{6}$	313-773	1	0.00057@458 K	[22]
Tm^{3+} , Yb^{3+} : $Na_3GdV_2O_8$	$^{1}G_{4}, ^{3}F_{3} \rightarrow {}^{3}H_{6}$	300-565	1	0.042@565 K	[23]
Tm³+, Yb³+:Bi ₂ WO ₆	$^{3}F_{3} \rightarrow ^{3}H_{6}$	298–573	0.00254@298 K	0.00144@298 K	This work
	$^3F_2 \rightarrow {}^3H_6$				
	³ F ₃ → ³ H ₆		0.167@573 K	0.0378@298 K	This work
Li ⁺ , Tm ³⁺ , Yb ³⁺ :Bi ₂ WO ₆	3 F ₃ \rightarrow 3 H ₆	298–573	0.00256@298 K	0.00162@298 K	This work
	F ₂ → T ₆ ³ F ₃ → ³ H ₆		0.196@548 K	0.0166@298 K	This work
Na ⁺ , Tm ³⁺ , Yb ³⁺ :Bi ₂ WO ₆	$^{3}F_{2}, ^{3}F_{3} \rightarrow ^{3}H_{6}$	298–573	0.003@298 K	0.0018@298 K	This work
	³ F ₃ → ³ H ₆		0.0977@548 K	0.046@298 K	This work
K ⁺ , Tm ³⁺ , Yb ³⁺ :Bi ₂ WO ₆	$^{3}F_{2}, ^{3}F_{3} \rightarrow ^{3}H_{6}$	298–573	0.00344@298 K	0.0024@298 K	This work
	$^3F_3 \rightarrow ^3H_6$ $^1G_4 \rightarrow ^3F_4$		0.476@548 K	0.0257@298 K	This work

samples. At 573 K, samples doped with 1% Li⁺ had Tm³⁺ thermally coupled energy level ${}^3F_3/{}^3F_2$ transitions to 3F_6 that produced red light emission at 685 and 705 nm higher than that of samples doped with Li⁺ at 298 K. The calculation results showed that the four Tm³⁺ emission peaks of the sample doped with 1% Li⁺, Na⁺, or K⁺ are derived from two-photon absorption processes. The relationship between the FIR of the Tm^{3+} thermally coupled energy levels ${}^3F_3/{}^3F_2$ and the temperature in the range of 298-573 K was calculated. At 298 K, the maximum relative temperature measurement sensitivities of the samples not doped with alkali metal ions and doped with 1% Li⁺, Na⁺, or K⁺ were 0.00144, 0.0016, 0.0024, and 0.0018 K⁻¹, respectively, and the maximum relative temperature sensitivity of the samples was improved after doping with 1% Li⁺, Na⁺, or K⁺. Under the same conditions, the relationship between the FIR of the Tm³⁺ nonthermally coupled energy levels ${}^{3}F_{3}/{}^{1}G_{4}$ and temperature was calculated for samples not doped with alkali metal ions and doped with 1% Li⁺, Na⁺, or K⁺, and the maximum relative temperature measurement sensitivity was 0.0378, 0.0166, 0.046, and 0.0257 K⁻¹, respectively, at 298 K. Obviously, compared with the characterization temperature of the thermally coupled energy levels ${}^{3}F_{3}/{}^{3}F_{2}$, the relative temperature measurement sensitivity of the nonthermally coupled energy levels ${}^{3}F_{3}/{}^{1}G_{4}$ increased by 26.3, 10.3, 19.1, and 13.9 times, respectively. In this work, the prepared 1% Na⁺, Tm³⁺, Yb³⁺:Bi₂WO₆ phosphors have a high maximum relative temperature measurement sensitivity, obtained by using the nonthermally coupled energy level ${}^3F_3/{}^1G_4$ FIR at 298 K. The fluorescence intensity ratios of 705 and 650 nm generated by the non thermally coupled energy levels ${}^{3}F_{3} \rightarrow {}^{3}H_{6}$ and ${}^{1}G_{4} \rightarrow {}^{3}F_{4}$ of Tm³⁺were used to obtain relatively high temperature sensitivity, which is more suitable for temperature sensing at room temperature.

Acknowledgments: This work was supported by the National Natural Science Foundation of China (No. 12164048).

Funding information: This research was funded by the National Natural Science Foundation of China (No. 12164048).

Author contributions: All authors have accepted responsibility for the entire content of this manuscript and approved its submission.

Conflict of interest: The authors state no conflict of interest.

Data availability statement: Data sharing is not applicable for this article. The data generated during the current study are available from the first author and corresponding author on reasonable request.

References

- [1] Wu, M., L. Yan, T. Wang, B. Zhou, and Q. Zhang. Controlling red color-based multicolor upconversion through selective photon blocking. *Advanced Functional Materials*, Vol. 29, No. 25, 2019, id. 1804160.
- [2] Zhang, Y., D. Liu, T. Wang, H. Jia, H. Liu, and Z. Fu. Upconversion luminescence and optical temperature sensing properties for Lu₂O₃Y₂O₃: Yb³⁺/Er³⁺/Gd³⁺ Phosphors. *Chinese Journal of Luminescence*, Vol. 40, No. 12, 2019, pp. 1478–1485 (in Chinese).
- [3] Huang, J., G. Tan, H. Ren, W. Yang, C. Xu, C. Zhao, et al. Photoelectric activity of a Bi₂O₃/Bi₂WO_{6-x}F_{2x} heterojunction prepared by a simple one-step microwave hydrothermal method. ACS Applied Materials & Interfaces, Vol. 23, 2014, pp. 21041–21050.
- [4] Thakur, H., A. Gathania, S. Kachahap, S. Singh, and R. Singh. Coprecipitation synthesis, structural and optical properties, and thermometry application of Tm³⁺/Yb³⁺ co-doped YPO₄ phosphor. *Journal of Luminescence*, Vol. 254, 2022, id. 119513.
- [5] Yin, X., Q. Xiao, L. Lv, X. Wu, X. Dong, Y. Fan, et al. Winning color-tunable upconversion luminescence and high-sensitive optical thermometry in K₃Gd(PO₄)₂: Yb³⁺, Er³⁺, Tm³⁺. Spectrochimica Acta Part A, Molecular and Biomolecular Spectroscopy, Vol. 291, 2023, id. 122324.
- [6] Zhang, Y., Y. Zheng, M. Liu, K. Wang, and H. Liu. Enhancement of the upconversion luminescence efficiency and temperature sensing property of Gd³⁺-doped BaWO4: Tm³⁺/Yb³⁺ phosphor. *Chinese Rare Earths*, Vol. 43, No. 2, 2022, pp. 99–107 (in Chinese).
- [7] Kumar A, S. Tiwari, A. Sardar, K. Kumar, and J. da Silva. Role of Ca²⁺ co-dopants on structural and optical properties of YF₃: Tm³⁺/Yb³⁺ upconversion phosphor for improved optical thermometry. Sensors & Actuators A Physical, Vol. 280, 2019, pp. 179–187.
- [8] Liu, X., X. Mi, Y. Guo, L. Lu, Q. Liu, Z. Bai, et al. Highly sensitive and near-infrared excitable optical thermometer based on CaGdAl₃O₇: Tm³⁺, Yb³⁺, Zn²⁺. *Journal of Alloys and Compunds*, Vol. 929, 2022, id. 167240.
- [9] Meng, M., R. Zhang, X. Fa, J. Yang, and J. Ou. Effect of Ce³⁺ Doping on upconversion luminescence of NaYF₄: Yb³⁺, Tm³⁺ nanoparticles and application of fluorescence temperature characteristics. *Chinese Journal of Luminescence*, Vol. 42, 2022, pp. 1763–1773 (in Chinese).
- [10] Yadav, R., S. Dhoble, and S. Rai. Enhanced photoluminescence in Tm³⁺ Yb³⁺, Mg²⁺ tri-doped ZnWO₄ phosphor: Three photon upconversion, laser induced optical heating and temperature sensing. Sensors and Actuators B Chemical, Vol. 273, 2018, pp. 1425–1434.
- [11] Guan, H., Y. Li. Na(Y_{1.5}Na_{0.5})F₆:RE³⁺ (Dy³⁺, Tb³⁺, Eu³⁺, Tm³⁺, Ho³⁺): controllable morphology, multicolor light and thermal properties. *Journal of Alloys & Compounds*, Vol. 859, 2021, id. 157833.
- [12] Wang, S., Q. Sun, B. Devakumar, J. Liang, L. Sun, and X. Huang. Novel Ca₂GdTaO₆: Mn⁴⁺, M (M = Li⁺, Na⁺, K⁺, and Mg²⁺) red phosphors for plant cultivation light-emitting diodes: Synthesis and luminescence properties. *Journal of Luminescence*, Vol. 214, 2019, id. 116525.
- [13] Tuo, J.,Y. Ye, H. Zhao, and L. Wang. Preparation and luminescence properties of Li⁺, Na⁺ co-doped (Y_xGd_yLu_{1-x-y})₂O₃: 0.5% Pr³⁺ Phosphors. *Chinese Optics*, Vol. 12, No. 6, pp. 1279–1287 (in Chinese).
- [14] Liu, G., L. Ding, and W. Zhang. Enhanced photoluminescence of Na⁺ -Doped Gd₂O₃: Sm³⁺ nanocrystals. *Chinese Journal of Luminescence*, Vol. 31, No. 5, 2010, pp. 706–710 (in Chinese).
- [15] Xu, W., X. Gao, L. Zheng, Z. Zhang, and W. Cao. An optical temperature sensor based on the upconversion luminescence from

- Tm³⁺/Yb³⁺ co-doped oxyfluoride glass ceramic. Sensors & Actuators B: Chemical, Vol. 173, 2012, pp. 250-253.
- [16] Shen, X., Y. Zhang, L. Xia, G. Yang, and Y. Zhou. Dual super broadband NIR emissions in Pr³⁺, Er³⁺, Nd³⁺ tri-doped tellurite glass, Ceramics International, Vol. 46, No. 9, 2020, pp. 14284-14286.
- [17] Zhou, H., W. Feng, Z. Zhang, Y. Zhang, and L. Ye. Upconversion Luminescence and Temperature Sensing Characteristics of Lu₂O₃: Er³⁺/Yb³⁺ Phosphor. *Chinese Journal of Luminescence*, Vol. 43, 2022, pp. 192-200 (in Chinese).
- [18] Zhang, N., H. Zhou, Y. Yin, T. Wang, J. Zhang, L. Ye, et al. Exploring promising up-conversion luminescence single crystal fiber in sesquioxide family for high temperature optical thermometry application. Journal of Alloys and Compounds, Vol. 889, 2021, id. 161348.
- [19] Zhang, Z., H. Zhou, F. Wu, Y. Zhang, and L. Ye. Temperature sensing characteristics of up-conversion luminescence in Tm³⁺/Yb³⁺ Co-

- doped LuYO₃ phosphor. Chinese Journal of Luminescence, Vol. 42, No. 12, 2021, pp. 1872-1881 (in Chinese).
- [20] Liu, Z., S. Long, Y. Zhu, W. Wang, and B. Wang. Optical thermometry based on thermolabile intrinsic polarons in Tm3+ and Yb3+ codoped congruent lithium niobate single crystal. Journal of Alloys and Compounds, Vol. 867, 2021, id. 158986.
- Ge, W., M. Xu, J. Shi, J. Zhu, and Y. Li. Highly temperature-sensitive and blue upconversion luminescence properties of Bi₂TiO₇: Tm³⁺/Yb³⁺ nanofibers by electrospinning. *Chemical Engineering* Journal, Vol. 391, 2019, id. 123546.
- [22] Zheng, L., Y. Li, H. Liu, X. Wei, and Z. Guo. Up-conversion luminescence and temperature characteristics of Tm³⁺, Yb³⁺ co-doped CaWO₄ polycrystal material, Acta Physica Sinica, Vol. 62, No. 24, 2013, pp. 108-113 (in Chinese).
- [23] Saidi, K., M. Dammak, K. Solercarracedo, and I. Martín. A novel optical thermometry strategy based on emission of $\mathrm{Tm^{3^+}/Yb^{3^+}}$ co-doped Na₃GdV₂O₈ phosphors. *Dalton Transactions*, 2022, Vol. 51, pp. 5108–5117.